

FRP-Confinement of Hollow Concrete Cylinders and Prisms

by R. Modarelli, F. Micelli, and O. Manni

Synopsis: The use of hollow-core reinforced concrete (RC) sections for bridge piers has become a popular engineering practice to obtain a reduction of the self-weight (especially in seismic zones) and a better structural efficiency in terms of the strength/mass and stiffness/mass ratios. In contrast to this popularity in practice, scientific studies on the mechanical behavior of such structural elements are limited.

The use of Fiber Reinforced Polymer (FRP) materials for external confinement of hollow core columns and piers is an almost unknown field at the moment. The research work presented herein aims at evaluating the influence of various experimental parameters on the effectiveness of FRP jackets applied to hollow concrete columns.

Hollow-core concrete prisms and cylinders were tested under uniaxial compression to study the stress-strain relationship before and after FRP jacketing. A range of experimental parameters were investigated: different concrete strength, type of fibers, number of wrap layers, column shape and dimensions, and for square and rectangular sections, the corner radius and the cross-sectional aspect ratio. Axial strain was measured by LVDTs, while strains in the fibers were recorded by electrical strain gauges.

Circular columns wrapped with FRP showed a significant increase in terms of both strength and ultimate displacements. Results obtained by laboratory tests were close to those recorded for FRP-confined concrete, which means that the increase in ultimate load was found to be comparable to that found in full circular sections. Rectangular columns showed a lower increase in ultimate capacity, compared to circular sections, even if the results related to ultimate axial displacement encourage adopting this technique for seismic retrofit to fulfill higher ductility requirements in both prismatic and cylindrical columns.

Keywords: FRP confinement; hollow-core columns; reinforced concrete

1030 Modarelli et al.

Rossella Modarelli is a senior researcher at the Materials and Structures Engineering Department for CETMA - Centre of Design, Styling and Materials Technologies, placed in Brindisi, Italy. Main research activities concern the rehabilitation and strengthening of concrete structures with FRP materials.

ACI Member **Francesco Micelli** is an Assistant Professor at the University of Lecce, Italy. He received his Ph.D. in Composites for Construction from the University of Lecce in 2003. He is currently active on ACI Committee 440. Principal scientific studies are in durability of FRP in civil engineering, strengthening and repair of concrete, wood and masonry structures with FRP composites.

Orazio Manni is research manager at the Materials and Structures Engineering Department for CETMA - Centre of Design, Styling and Materials Technologies, placed in Brindisi, Italy. He received his Ph.D. in Composites for Civil Engineering from the University of Lecce in 2000. Main research interests include mechanical behaviour of concrete and masonry structures reinforced with FRP and technology transfer from aeronautical technologies to civil engineering, regarding the use of composite materials.

INTRODUCTION

A large number of experimental studies demonstrated the structural efficiency of FRP-confinement for RC columns, assuming a modified constitutive-law for confined concrete^[1-4]. Numerical modeling was developed to predict the stress-strain behavior of concrete after FRP wrapping^[5-8] and recommendations were furnished to practitioners for design of FRP-retrofitted RC columns^[9-11].

Research related to the use of FRP-confinement of hollow-core RC columns is very scarce at the moment; a few data reporting properties of RC hollow-core columns under seismic forces are available. This does not result in accordance with the thousand of applications all over the world in which bridge piers are designed as hollow-core columns to maximize structural efficiency in terms of strength/mass and stiffness/mass ratios. A recent study^[12] reports the behavior of hollow rectangular bridge columns confined with CFRP straps under axial compression and cyclic flexure. Obtained results encourage the use of FRP composites for seismic retrofit, since the ductility factor increased for FRP-confined columns respect to control specimens. Even if the ductility was higher, the increase was not proportional respect to the increasing amount of FRP sheets. FRP straps also reduced the presence of shear cracks, changing the failure mode from shear to flexural collapse. This problem was also discussed in^[13] where the results of cyclic flexural tests on compressed hollow-core rectangular RC columns showed shear failure in concrete without appropriate transverse arrangement.

The objective of the research presented herein was to investigate the stress-strain behavior of hollow-core FRP-confined concrete under compressive load, since it was found that confinement acts as strengthening system either for compressed columns that may be subjected to cyclic flexural forces, or dynamic compressive actions generated by seismic events. The behavior of FRP-wrapped concrete can be used to study how confinement influences the moment-curvature (ductility) relationships and shear behavior under cyclic forces. Then it is useful to know how the presence of FRP confining jackets

increases the compressive strength especially in those cases that show inadequate transverse reinforcement (spiral or stirrups) in bearing dynamic compression forces (Figure 1).

The results of this research furnish useful information regarding the behavior of hollow-core concrete columns confined with FRP under monotonic compression, respect to important variables which are concrete strength, aspect ratio and shape of the cross section, type of FRP material, construction details such as corner radius of prismatic columns.

EXPERIMENTAL PROGRAM

Materials

A total of 124 specimens were tested, which included 85 specimens wrapped with FRP and 39 plain concrete specimens. Two different kind of concrete mix have been realized to investigate the influence of the concrete strength: the former had the ratios of water/cement, sand/cement, gravel/cement of 0.7, 3.8, 2.4, respectively, the latter 0.5, 2.5, 1.7. The coarse aggregate consisted of crushed stone with a maximum size of 9 mm.

All specimens were cured for 60 days at a temperature of 20°C and a relative humidity that exceeded 60%. The average 28-day compressive strength of the two kinds of concrete were 28 MPa and 38 MPa respectively.

The concrete specimens were wrapped with unidirectional CFRP and GFRP composites with fibers aligned at 90° respect to the principal axis of the specimen. The experimental properties of the composites sheets and the epoxy resin system are reported Table 1. Table 2 summarizes the specimens involved in the experimental program. The specimen designation can be interpreted as follows: the first letter represents the FRP material (“C” for CFRP and “G” for GFRP, with “N” signifying absence of FRP confinement), followed by the specimen geometry “C” or “P” (cylinder or prism).

Test set up

Unidirectional fibre sheets were applied using a manual wet lay-up process under the same thermal and hygrometric conditions. For small scale specimens (300 mm high) load was applied with a 3000-kN compression machine (Figure 2a) and measured by means of a pressure transducer. Two LVDTs were used to monitor the relative displacement between the extreme faces of the specimen, and, from it, the average axial strain at each load level. Three strain gauges were applied on each cylinder at mid-height in the hoop direction. Specimens that were higher than 300 mm have been loaded using a manual pump (Figure 2b), applied force was measured using a load cell of 2000 kN capacity, five strain gauges were used to monitor the strain in the fibers, two LVDTs were used to measure the axial displacement. Location of electrical strain gauges and the main geometrical characteristics are shown in Figure 3. In order to avoid that the axial load be applied directly on the fibers, the FRP wrap did not cover the full height of the cylinder; instead, a narrow gap was left between the end concrete surfaces and the extreme composite fibers. Direct axial loading of the FRP may result in local buckling of the composite in the axial direction close to the loaded surfaces. The buckling portions expand outward, which results in less contact pressure with concrete. Therefore, direct loading of the FRP should yield a lower confinement effectiveness.

RESULTS AND DISCUSSION

Collapse of FRP-wrapped specimens was due to fibers rupture; failure occurred in a sudden and explosive way and was only preceded by typical creeping sounds. Cylindrical and prismatic specimens after failure are shown in Figure 4; fibre rupture in prismatic columns occurred close to the corner regions, as expected from theoretical considerations, then delamination spread towards the entire section.

In Table 3 the average experimental results are summarized; the increase in terms of compressive strength (f'_{cc}/f'_c where f'_{cc} and f'_c are the compressive strength of the confined and unconfined concrete specimens, respectively) and ductility (ϵ_{cc}/ϵ_c where ϵ_{cc} and ϵ_c are the axial strains at peak stress of the confined and unconfined concrete specimens, respectively), intended as capacity in terms of ultimate axial displacement, are shown in the same table. It is evident that in all cases the presence of external FRP jackets increased the mechanical properties of plain concrete, in different amount according to the number of FRP layers, concrete properties and cross section geometry.

Representative stress-strain curves for each series of FRP-wrapped specimens, grouped together according to the cross section shape, are reported in Figure 5 for concrete cylinders and in Figure 6 for concrete prisms.

In the following paragraphs, all the parameters considered in this experimental study are analyzed.

Cross section's shape

Circular sections -- For circular full-core sections stress-strain curves of FRP confined concrete are bilinear with a transition zone (see Figure 5a), as expected from theoretical considerations. The first slope of the curve (i.e. the one of the initial elastic zone) is not substantially altered by the presence of FRP, as the confined and the unconfined specimens behave in the same manner, irrespective of the number of layers. The strengthening effect of the FRP layers begins only after the concrete has reached the unconfined strength, at this stage transversal strains activate the confining pressure of FRP. In this region little increases of load produce large lateral expansions, and consequently an increasing confining pressure, due to the elastic behavior of FRP materials. In the case of circular sections the section is fully confined, therefore the second slope is positive, showing the capacity of confining pressure to limit the effects of the deteriorated concrete core, which allows reaching higher stresses.

The same behavior is shown by circular section with low dimensions of the hollow-core and lower concrete strength (series CC2 and CC3 in Figure 5b).

The curves are different in the case of higher concrete strength (series CC6 and CC7 in the same figure). The first slope does not change, while the second one has lower slope, due to the damaged concrete in the interior side of the wall thickness, which does not receive the confinement action of the FRP.

When the dimensions of the hollow core increase, in the case of low concrete strength (series CC8, CC9 and CC10 in Figure 5c), the initial slope remains unchanged also after the reaching of the maximum stress of unconfined concrete. The second branch is almost a plateau with null slope, due to damage occurred inside those regions that are not affected by strengthening action of FRP. Spalled concrete was observed inside the hollow core after test. Significant increases of both strength and deformation capacities have been measured (Table 3). For higher concrete strength (series CC11 and CC12 in Figure

65d) the behavior is similar to the previous, except for the fact that second branch is descendent. This may be explained by the fact that different cracking behavior of stronger concrete generated expulsion of concrete from the wall thickness to the hollow core at different stress levels. This phenomenon reduced the ductility of the confined specimens that showed lower values of maximum axial displacement.

It should be noted also that the transition region in diagrams of Figure 5c and Figure 5d is visible for values of compressive stress that are remarkably higher respect to maximum strength of plain concrete. Thus it is clear that action of FRP jacket in this case may increase the service load of the compressed element since the first linear region is strongly extended.

Square and rectangular sections -- Prismatic specimens with full concrete core showed typical stress-strain behavior with a first linear branch of the curve, followed by a plateau corresponding to the confining action of the FRP. In Figure 6a, related to square sections, it is evident that confinement is less effective than circular sections (Figure 5a), due to the unconfined regions far from the corners. Different slopes and effectiveness of confinement in terms of ultimate load are mostly related to different corner radius as discussed later.

Figure 6b shows the curves for FRP-confined columns with hollow core square cross section and different concrete strength. The slope of the first linear region is affected by the different stiffness of concrete. A second branch with slope close to zero testifies the confinement activated in the regions close to the corners of the prism. In conclusion, similar behavior was observed between prisms and hollow-core prisms with square section (see also Table 3).

Figure 6c illustrates the curves for prisms with rectangular section strengthened with different amount of FRP (effects of FRP amount will be discussed in the following).

In Figure 6d correspondent curves are reported for hollow-core rectangular sections. It is evident that a decrease was observed in the slope of the second branch of the curve, after incipient crushing of concrete core, even if effectiveness of confinement in terms of strength and ductility shows to be the same. This behavior is due to the presence of a wall thickness that produce a softening behavior different from that of a full concrete core that remains totally wrapped in the FRP jacket, while the hollow core produces concrete spalling in the unstrengthened regions.

The effect of slenderness in terms of higher column and lower wall thickness (larger hollow-core region) is presented in Figure 6e that shows that the effectiveness of FRP confinement decreases in terms of compressive strength and ultimate displacement respect to circular and square columns. This means that confinement of hollow-core sections produces almost the same effects of full-core sections for circular and square sections, while increase in strength and ductility for rectangular sections with high aspect ratio and high hollow-core volume reduce dramatically for low amount of FRP wraps.

Effect of corner radius

Two corner radius have been considered. For the series CP1, the specimens have been cast with a corner radius of 10 mm, which is representative of columns for which a minimum of preparation is done. The specimens of the series CP3 have been realized with a corner radius of 25 mm, to represent concrete element correctly prepared. The

1034 Modarelli et al.

radius of the corners was obtained directly by casting concrete in steel formworks with rounded corners according to design specifications.

The analysis of stress-strain curves of sharp-edged confined elements (see Figure 7) shows that the geometry of the cross section does not allow the CFRP wrap to develop a significant confining pressure since fibers are prone to premature rupture. Thus corner radius of square and rectangular sections has a fundamental importance for confinement effectiveness, in fact the increase of load capacity was of 128% for the specimens of the series CP1; while this increment has been remarkably higher for the series CP3 being equal to 196%, respect to plain concrete.

Effect of the concrete strength

The influence of the concrete strength has been investigated on three different kinds of circular geometry: small section (diameter $D=150\text{mm}$), small hollow section (diameter $D=150\text{mm}$, hollow diameter $\Phi=50\text{mm}$), and big hollow section (diameter $D=250\text{mm}$, hollow diameter $\Phi=150\text{mm}$). Fixed the geometry and the FRP strengthening ratio, the specimens have been realized with different concrete strength (28 MPa and 38 MPa). In Table 4 the increases in terms of strength and ductility for each series are reported.

As can be observed in Figure 8, the increase of load capacity is always higher for the lower concrete strength than the one found for the higher concrete strength. This effect is even more evident on the deformations (Figure 9). It has been confirmed that the effect on the bearing and deformation capacities decreases with increasing concrete strength, as found by other authors. Mechanical effects caused by the different concrete quality are also evident in the first branch of the curves, where stronger concrete shows higher stiffness respect to concrete with lower strength (see Figure 10).

Effect of FRP strengthening ratio

The effect of FRP amount has been studied on small circular hollow sections (series CC2-CC3-CC4, CC6-CC7, CC8-CC9-CC10, CC1-CC12), square sections (series CP2-CP3,) and rectangular sections (series CP6-CP7, CP10-CP11, CP15-CP16). Figure 11 shows the comparison between the tested specimens respect to the number of FRP sheets. In all cases (see Table 5) the increase of the numbers of sheets generated not only a larger increase of compressive strength, but also a remarkable increase of deformation capacity. However the increase of the strengthening ratio is not able to modify the slope of the last branch of the stress-strain curve (Figure 11b, c, e, f), except in the case of little hollow-core dimensions (series CC2-CC3-CC4, series CC6-CC7, series CP2-CP3 in Figure 11a, d).

Effect of type of fibers

The specimens CC1 and CG1 have been confined with CFRP and GFRP respectively. Even if glass fibers have lower tensile strength and modules respect to carbon fibers used in this study, thickness of GFRP was about two times that of CFRP. Thus the strengthening ratio was almost the same in the two cases. Stress strain curves showing comparison between GFRP and CFRP confined cylinders are illustrated in Figure 12. As expected from design equations the compressive strength was almost the same between CFRP and GFRP confined cylinders. Axial strain resulted higher for CC1 specimens

even if it was expected a larger displacement using GFRP sheets, due to the higher ultimate strain of glass fibers under tensile loads.

CONCLUSIONS

A large experimental program has been presented to study the behavior of FRP-confined concrete under compressive loads, respect to the presence of hollow core inside the cross section, different concrete strength, different geometry and shape of cross section, different corner radius of prismatic columns, different type of fibers.

A total of 124 small scale and half scale column specimens were tested, important remarks are reported in the following.

- FRP-confinement revealed to be effective for hollow-core concrete sections, even if the increase of strength and ductility decreased from circular to square and rectangular sections, as same as for full-core columns.
- Higher concrete strength decrease the effect of FRP confinement, it was seen that different cracking behavior at high loads generated different concrete spalling inside the hollow core.
- Higher amount of FRP sheets is not able to modify the slope of the last branch of the stress-strain curve, except in the case of little hollow-core dimensions.
- Dimensions of corner radius in prismatic columns had a significant influence in terms of ultimate strength and displacement, increase of 50% were observed from $R_c=10$ mm to $R_c=25$ mm. It is always recommended to avoid corners without rounded surface since the confined region reduces dramatically, with high stress-concentration in FRP close to the corner.

REFERENCES

- [1] Harajli MH and Rteil AA, "Effect of Confinement Using Fiber-Reinforced Polymer or Fiber-Reinforced Concrete on Seismic Performance of Gravity Load-Designed Columns", *ACI Struct. Journ.*, Vol. 101, Issue 1, 2004, pp. 47-56.
- [2] Rochette P and Labossière P, "Axial Testing of Rectangular Column Models Confined with Composites", *ASCE -J. Compos. for Constr.*, Volume 4, Issue 3, 2000, pp. 129-136.
- [3] Teng JG and Lam L, "Compressive Behavior of Carbon Fiber Reinforced Polymer-Confined Concrete in Elliptical Columns", *ASCE - J. Struct. Engrg.*, Volume 128, Issue 12, 2002, pp. 1535-1543.
- [4] Campione G, Miraglia N, Papia M, Influence of section shape and wrapping technique on the compressive behaviour of concrete columns confined with CFRP sheets, *Proceedings of CCC2003 - Composites in Construction Int. Conf.*, September 16-19 2003, Cosenza, Italy, 301-306.
- [5] Spoelstra MJ, Monti G, FRP-Confined concrete model, *ASCE -J. Compos. Constr.* 1999; 3(3): 143-150.

1036 Modarelli et al.

[6] Toutanji HA, Stress-strain characteristics of concrete columns externally confined with advanced fiber composites sheets, *ACI Mat. J.* 1999; 96 (3): 397-404.

[7] Samaan M, Mirmiran A, Shahawy M, Model of concrete confined with fiber composites, *ASCE- J. Struct. Eng.* 1998:124 (9), pp. 1025, 1031.

[8] Wu G, Wu Z, Lu Z, Stress-strain relations for FRP-confined concrete prisms, *Proceedings of FRPRCS-6 Int. Conf.*, July 8-10 2003, Singapore, 561-570

[9] FIB TG 9.6, *Externally Bonded FRP Reinforcement for RC Structures*, Technical report 138 pp., October 2001.

[10] ACI Committee 440, *Design and Construction of Externally Bonded FRP Systems for Strengthening Concrete Structures* - ACI 440.2R.02, 45 pp., July 2002.

[11] Japan Society of Civil Engineers (JSCE), *Recommendations for Upgrading of Concrete Structures with Use of Continuous Fiber Sheets*, Concrete Engineering series 41, Ed. K. Maruyama, 88 pp., March 2001.

[12] Mo YL, Yeh YK and Hsieh DM, "Seismic retrofit of hollow rectangular bridge columns", *Columns*", *ASCE - J. Composit. for Constr.*, Volume 8, Issue 1, 2004, pp. 43-51.

[13] Takahashi Y and Iemura H, "Inelastic Seismic Performance of RC Tall Piers with Hollow Section", *Proceedings of 12th World Conference on Earthquake Engineering*, No.1353, 2000/2, New Zealand.

Table 1 – Mechanical properties of FRP fibers and epoxy system

	Thickness (mm)	Young modulus (GPa)	Tensile strength (MPa)	Ultimate strain (%)
CFRP	0.165	221	3068	1.40%
GFRP	0.23	86	1957	2.28%
Epoxy	----	3	50	2.50%

Table 2 – Experimental program

Specimen designation	Number of specimens	Nominal dimensions Length x Diameter (mm)	Hollow core dimensions (mm)	Confinement material	Concrete strength (MPa)	Number of plies
NC1	3	300x150	--	None	28	0
CC1	3	300x150	--	CFRP		1
CG1	3	300x150	--	GFRP		1
NC2	3	300x150	50	None		0
CC2	3	300x150	50	CFRP		1
CC3	3	300x150	50	CFRP		2
CC4	3	300x150	50	CFRP		3
NC5	3	300x150	--	None	38	0
CC5	3	300x150	--	CFRP		1
NC6	3	300x150	50	None		0
CC6	3	300x150	50	CFRP		1
CC7	3	300x150	50	CFRP	2	
NC8	3	500x250	150	None	28	0
CC8	3	500x250	150	CFRP		1
CC9	3	500x250	150	CFRP		2
CC10	3	500x250	150	CFRP	38	3
NC11	3	500x250	150	None		0
CC11	3	500x250	150	CFRP		1
CC12	3	500x250	150	CFRP	2	
NP1	3	300x150x150	--	None	28	0
CP1	3	300x150x150	--	CFRP		2
NP2	3	300x150x150	--	None		0
CP2	3	300x150x150	--	CFRP		1
CP3	3	300x150x150	--	CFRP	38	2
NP4	3	300x150x150	50	None		0
CP4	3	300x150x150	50	CFRP		2
NP5	3	300x150x150	50	None		0
CP5	3	300x150x150	50	CFRP		2
NP6	3	400x200x150	--	None	28	0
CP6	3	400x200x150	--	CFRP		1
CP7	3	400x200x150	--	CFRP		2
CP8a	2	400x200x150	--	IBRID-1		3
CP8b	1	400x200x150	--	IBRID-2		5
CP9	3	400x200x150	--	GFRP		2
NP10	3	400x200x150	100x50	None		0
CP10	3	400x200x150	100x50	CFRP		1
CP11	3	400x200x150	100x50	CFRP		2
CP12	2	400x200x150	100x50	IBRID-1		3
CP13	2	400x200x150	100x50	IBRID-2		5
CP14	3	400x200x150	100x50	GFRP		2
NP16	3	600x300x150	200x50	None		0
CP16	3	600x300x150	200x50	CFRP		1
CP17	3	600x300x150	200x50	CFRP		2

Table 3 – Experimental results

Specimen designation	Confinement material	Number of plies	Compressive strength (MPa)	Axial strain (%)	Hoop strain (%)	$\frac{f'_{cc}}{f'_c}$	$\frac{\varepsilon_{cc}}{\varepsilon_c}$
NC1	None	0	28,35	0,49	0,17	-	-
CC1	CFRP	1	55,25	2,20	1,53	1,95	4,50
CG1	GFRP	1	53,27	1,90	4,98	1,88	3,88
NC2	None	0	24,03	0,38	0,05	-	-
CC2	CFRP	1	45,15	2,25	1,22	1,88	5,90
CC3	CFRP	2	50,79	2,55	0,65	2,11	6,68
CC4	CFRP	3	80,02	3,09	0,73	3,33	8,07
NC5	None	0	38,24	0,63	0,39	-	-
CC5	CFRP	1	62,73	1,49	1,32	1,64	2,38
NC6	None	0	35,05	0,47	0,40	-	-
CC6	CFRP	1	47,87	1,53	1,23	1,37	3,29
CC7	CFRP	2	59,19	1,71	0,77	1,69	3,67
NC8	None	0	11,37	0,49	0,34	-	-
CC8	CFRP	1	26,59	1,58	0,28	2,34	3,23
CC9	CFRP	2	34,11	1,65	0,22	3,00	3,36
CC10	CFRP	3	35,99	2,24	0,18	3,16	4,57
NC11	None	0	13,91	0,62	0,84	-	-
CC11	CFRP	1	31,89	1,22	0,48	2,29	1,98
CC12	CFRP	2	39,02	1,50	0,15	2,81	2,44
NP1	None	0	25,04	0,63	0,67	-	-
CP1	CFRP	2	31,99	3,57	1,23	1,28	5,67
NP2	None	0	21,43	0,56	0,84	-	-
CP2	CFRP	1	36,18	1,83	1,40	1,69	3,25
CP3	CFRP	2	42,06	3,11	1,48	1,96	5,52
NP4	None	0	16,90	0,46	1,34	-	-
CP4	CFRP	2	39,38	2,40	0,87	2,33	5,16
NP5	None	0	27,37	0,46	0,68	-	-
CP5	CFRP	2	48,46	2,24	0,92	1,77	4,91
NP6	None	0	17,58	0,88	0,45	-	-
CP6	CFRP	1	30,25	2,36	1,56	1,72	2,69
CP7	CFRP	2	34,11	3,26	1,45	1,94	3,72
CP8A	IBRID-1	3	38,49	4,81	0,81	2,19	5,48
CP8B	IBRID-2	5	53,56	4,96	1,62	3,05	5,66
CP9	GFRP	2	32,24	2,90	1,58	1,83	3,31
NP10	None	0	22,89	1,07	0,29	-	-
CP10	CFRP	1	21,83	1,92	0,84	0,95	1,79
CP11	CFRP	2	29,93	2,69	0,52	1,31	2,50
CP12	IBRID-1	3	34,24	3,57	1,01	1,50	3,32
CP13	IBRID-2	5	36,30	4,09	0,54	1,59	3,81
CP14	GFRP	2	23,34	3,05	0,73	1,02	2,85
NP15	None	0	13,36	0,38	0,07	-	-
CP15	CFRP	1	22,76	1,17	0,08	1,70	3,11
CP16	CFRP	2	24,22	1,98	0,05	1,81	5,27

Table 4 – Increase of strength and ductility of FRP-confined cylinders with different concrete strength

Label	Nominal dimen. (mm)	Concrete strength (MPa)	Hollow (mm)	n	f'_{cc} (MPa)	Axial strain (%)	Hoop strain (%)	$\frac{f'_{cc}}{f'_c}$	$\frac{\epsilon_{cc}}{\epsilon_c}$
CC1	300x150	28	0	1	55,25	2,20	1,53	1,95	4,50
CC5	300x150	38	0	1	62,73	1,49	1,32	1,64	2,38
CC2	300x150	28	50	1	45,15	2,25	1,22	1,88	5,90
CC6	300x150	38	50	1	47,87	1,53	1,23	1,37	3,29
CC3	300x150	28	50	2	50,79	2,55	0,65	2,11	6,68
CC7	300x150	38	50	2	59,19	1,71	0,77	1,69	3,67
CC8	500x250	28	150	1	26,59	1,58	0,28	2,34	3,23
CC11	500x250	38	150	1	31,89	1,22	0,48	2,29	1,98
CC9	500x250	28	150	2	34,11	1,65	0,22	3,00	3,36
CC12	500x250	38	150	2	39,02	1,50	0,15	2,81	2,44

Table 5 – Effect of FRP strengthening ratio

Specimen designation	Confinement material	Number of plies	Compressive strength (MPa)	Axial strain (%)	Hoop strain (%)	$\frac{f'_{cc}}{f'_c}$	$\frac{\epsilon_{cc}}{\epsilon_c}$
CC2	CFRP	1	45,15	2,25	1,22	1,88	5,90
CC3	CFRP	2	50,79	2,55	0,65	2,11	6,68
CC4	CFRP	3	80,02	3,09	0,73	3,33	8,07
CC6	CFRP	1	47,87	1,53	1,23	1,37	3,29
CC7	CFRP	2	59,19	1,71	0,77	1,69	3,67
CC8	CFRP	1	26,59	1,58	0,28	2,34	3,23
CC9	CFRP	2	34,11	1,65	0,22	3,00	3,36
CC10	CFRP	3	35,99	2,24	0,18	3,16	4,57
CC11	CFRP	1	31,89	1,22	0,48	2,29	1,98
CC12	CFRP	2	39,02	1,50	0,15	2,81	2,44
CP2	CFRP	1	36,18	1,83	1,40	1,69	3,25
CP3	CFRP	2	42,06	3,11	1,48	1,96	5,52
CP6	CFRP	1	30,25	2,36	1,56	1,72	2,69
CP7	CFRP	2	34,11	3,26	1,45	1,94	3,72
CP10	CFRP	1	21,83	2,00	0,84	0,95	1,80
CP11	CFRP	2	29,93	2,69	0,52	1,31	2,42
CP15	CFRP	1	22,76	1,18	0,08	1,70	3,14
CP16	CFRP	2	24,22	1,98	0,05	1,81	5,27



Figure 1– Crushed RC column under seismic loads

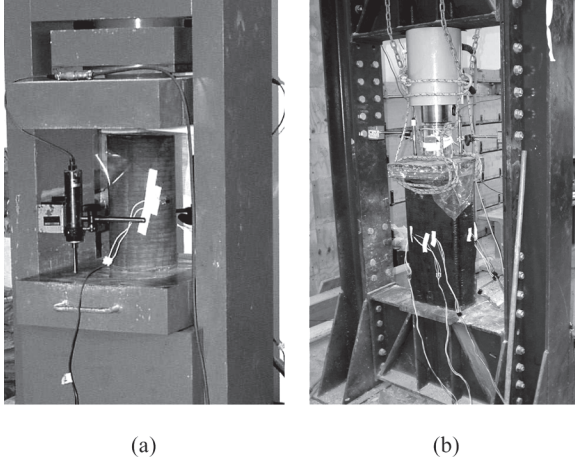


Figure 2 – Test set-up

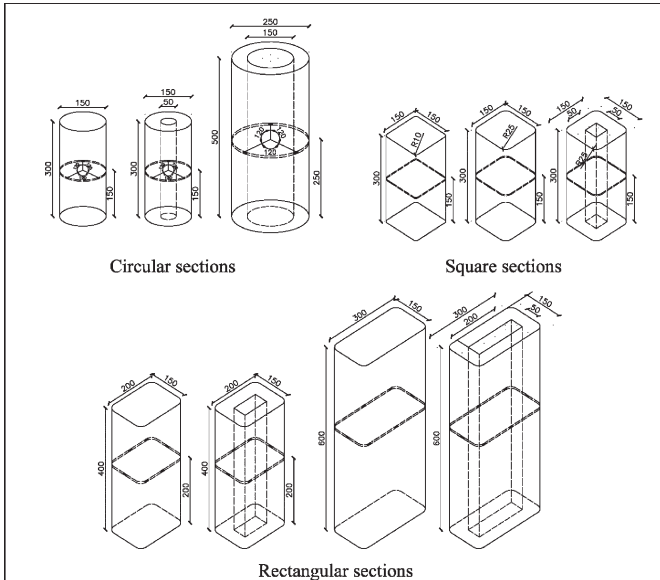


Figure 3 – Geometry of specimens



Figure 4 – Failure of FRP- wrapped specimens

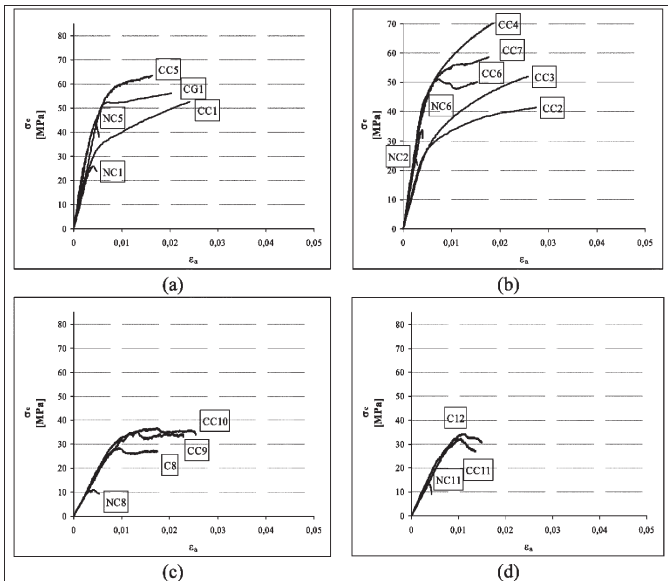


Figure 5 – Stress-strain curves of FRP-confined cylinders

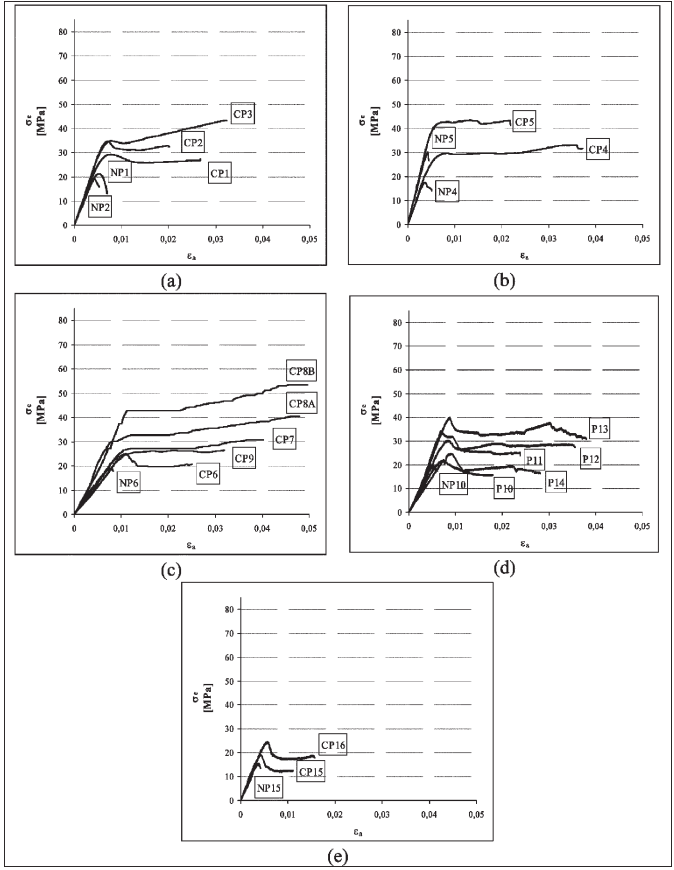


Figure 6 – Stress-strain curves of FRP-confined prisms

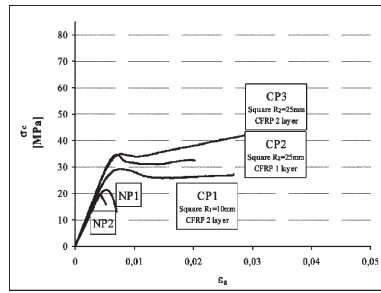


Figure 7 – Effects of the corner radius

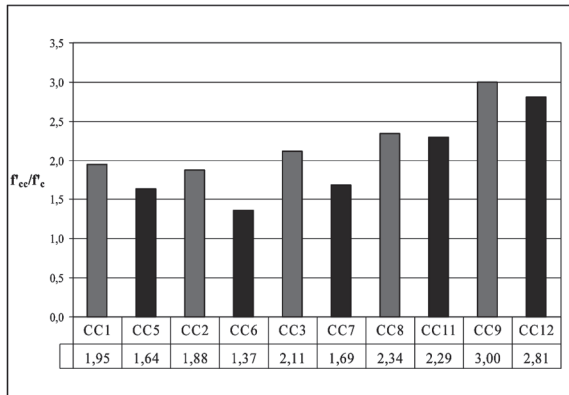


Figure 8 – Increase of strength of FRP-confined cylinders with different concrete strength

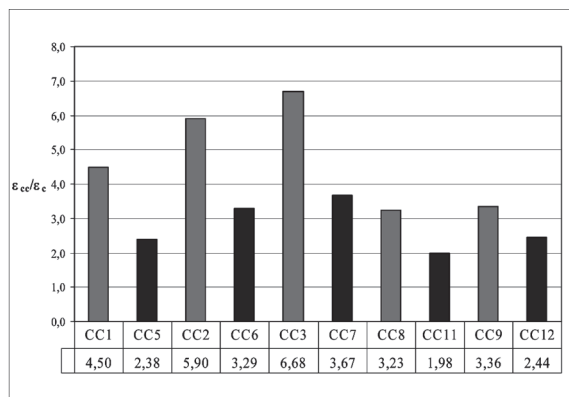


Figure 9 – Increase of ductility of FRP-confined cylinders with different concrete strength

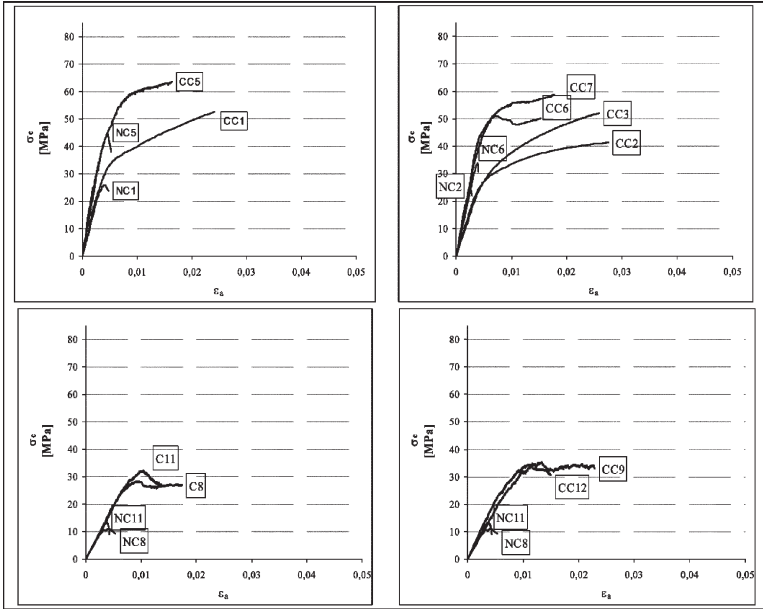


Figure 10 – Stress-strain curves of FRP-confined cylinders with different concrete strength

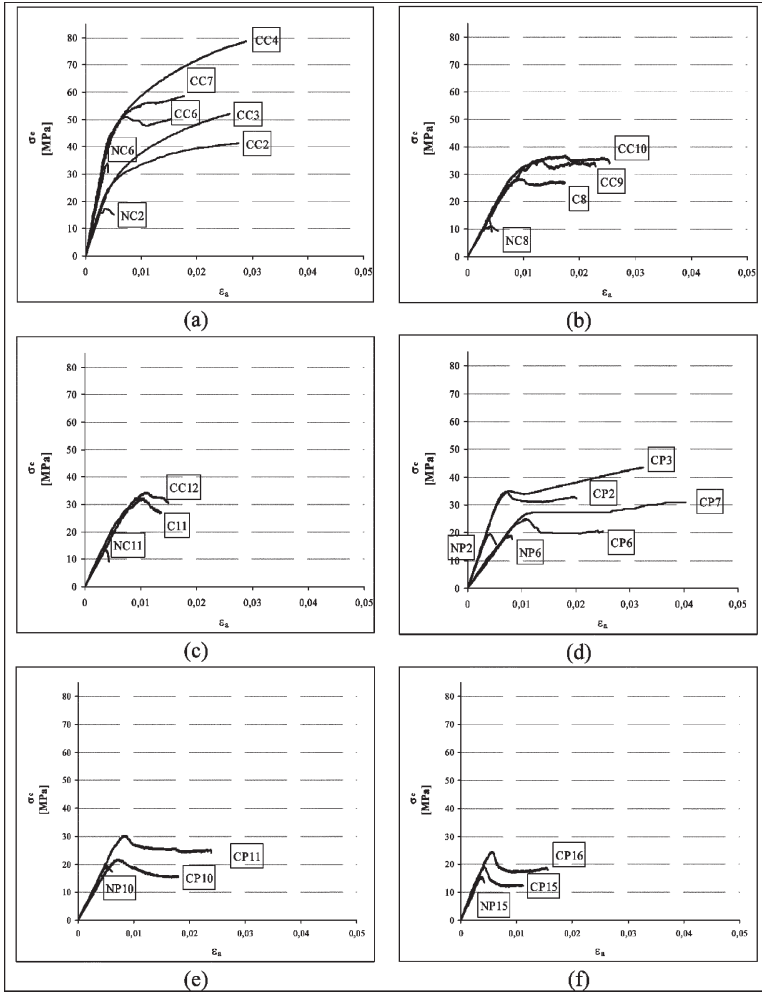


Figure 11 – Stress-strain curves of FRP-confined cylinders and prisms with different strengthening ratio

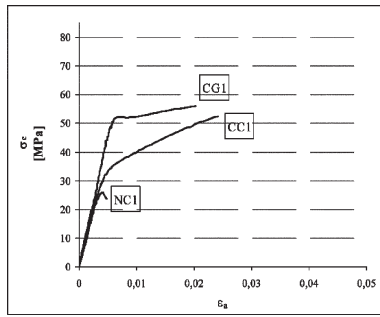


Figure 12 – Behavior of GFRP and CFRP-confined cylinders